Available online at: http://www.basra-science-journal.org

ISSN –1817 –2695

Received 1-12-2014, Accepted 24-3-2015

Photoionization, Electron-Ion Recombination and Recombination Rates of N^{+1} and Al^{+3} ions using Relativistic Dirac R-matrix Method

A.H.Hussain A.A.Khalaf F.A.Ali

University of Basrah , College of Science, Department of Physics , IRAQ
e.mail : akeel_hashem74@yahoo.com

Abstract

The bound states, photoionization,electron-ion recombination and recombination rates of N^{+1} and Al^{+3} ions are investigated using the fully relativistic R-matrix method . These processes are fundamental atomic processes in astrophysical plasmas. In most existing astrophysical models these atomic data are from methods that do not sufficiently consider the level of complexity attributed to the large number of autoionizing resonances that manifest themselves in the photoionization cross-sections and, consequently, in the inverse process of (electron-ion) recombination.The Dirac Atomic R-matrix Code has been extended from low-energy electron scattering to handle bound states, photoionization and radiative recombination .In the relativistic R-matrix calculations,the orbitals are obtained from the multiconfiguration Dirac-Fock method by using GRASP code,where in this method ,an atomic state is approximated by a linear combination of configuration state functions of the same symmetry.The configuration state functions are antisymmetrized products of a common set of orthonormal orbitals which are optimized on the bases functions of Dirac-Coulomb Hamiltonian.This basis is used to obtain bound orbitals from which the target ions are constructed in DARC code .Further relativistic contributions to the atomic states due to Breit interactions are added by diagonalizing the Dirac-Coulomb-Breit Hamiltonian matrix.The dominant quantum electrodynamic contibutions have also been included as a perturbation.Calculations have been performed on N^{+1} and Al^{+3} ions.Where good agreement is obtained between the results in this paper with the results of others.

Keywords: Photoionization; e-ion recombination; Dirac equations ; relativistic R-matrix method

1.Introduction

During the last years, there has been renewed interest in the photoionization and other radiative processes of atoms and their ions. This interest is, on the one hand, due to the desire of understanding the fundamental atomic processes, on the other hand, due to the need of practical applications in the plasma physics.West[1] gave a review on the development of both theoretical and experimental works on photoionization of atomic ions over the last 25 years. Opacity project[2-3] obtained a large amount of radiative atomic data to calculate the radiative opacity of the astrophysical plasmas. Collisions of electrons and photons with atoms and ions are among the most elementary processes that can be studied within the framework of quantum mechanics. The latter processes include elastic scattering, inelastic excitation, and ultimately collisional break-up in ionization. These collisions determine to a considerable extent the energy balance for different plasma and laser devices, while the understanding of the underlying mechanisms allows one to study comprehensively the properties of atomic systems and their structure. Benchmark experiments and calculations have further advanced our basic knowledge of this field, while at the same time providing urgently needed input data for modeling programs describing astrophysical and laboratory plasmas, planetary atmospheres, and lasers. Due to the many difficulties associated with experimental investigations of these collisions, such as the normalization of absolute cross sections and low count rates, and also due to the enormous amount of data needed for the modeling programs, the vast majority of currently available input data for these programs consists of theoretical predictions[4].During the last years, there has been renewed interest in the photoionization and radiative recombination of atoms and their ions.The photoionization of atomic systems, one of the fundamental processes of nature, also has a myriad of applications to other branches of physics, to other sciences, and to technology generally. Thus, for both basic and applied reasons, atomic photoionization has been of interest for a very long time, even in the era before Einstein's explanation of the photoelectric effect in 1905[5].With the development of quantum mechanics early in the twentieth century came calculations of the photoionization process. These calculations were at the simple analytic hydrogenic [6] and Born approximation level [7] until the 1950s when calculations using more realistic central-field or Hartree–Fock wave functions [8] were employed. Then from the late 1960s, a variety of methods for the calculation of atomic photoionization were developed, which attempted to include, at some level of approximation, the many-body interactions among the electrons of the atom in both the initial (discrete) and final (continuum) states of the photoionization process, i.e. electron correlation[9].The photoionization process is also important in high temperature plasma devices, such as controlled thermonuclear fusion reactors[10], and particularly in high-density inertially confined plasmas[11].Also the Photoionization process is considered to be a useful method to carry out spectroscopical and dynamical investigations on atomic systems, as the information thus obtained is of relatively pure form. This is simply because the photon field couples very weakly with the system to induce minimal perturbation. Moreover, since the final channel comprises of only the photoelectron, the incoming photon being absorbed by the target, the analysis becomes rather simple.Over the last several decades there have been many experimental studies [12] on atomic photoionization to understand the dynamics of the process. In recent times, owing to the advent of experimental technology, a renewed interest is seen in high precision measurements.For a long time, the main obstacle to extensive experimental research at energies as low as

x-ray range has been the limitation of discrete characteristic lines from x-ray tubes. Currently available x-ray synchrotron radiation facilities remove this obstacle and provide the experimentalists with an intense, tunable, and highly polarized x-ray beam[13].Since The R-matrix method has proved to be a remarkably stable, robust and efficient technique for solving the close-coupling equations that arise in electron and photon collisions with atoms and ions [14-16] , in this work the Dirac atomic R- matrix method has been adopted to calculate bound states and the process of photoionization , radiative recombination and recombination rates of N^{+1} and Al^{+3} ions . Multiconfigurational Dirac-Fock atomic structure calculations are used to obtain the target models for R-matrix calculations. The low photoelectron energy range that this approximation is applicable to is generally similar to that of the energy levels of the target used in the problem.

R-matrix theory was first introduced in nuclear physics by Wigner [17-18].Around the early 1970s it was realised that this approach could also be used in atomic and molecular physics[19].During the past thirty-five years a series of related R-matrix methods have been published periodically.Building on the important foundational work of Allison [20], Burke [21], Hibbert [22] and Robb [23,24], Berrington et.al. published in 1974 [25] and again in 1978 [26] an influential general program based on the non-relativistic Hamiltonian for calculating electron–atom and electron–ion cross sections as well as general atomic and photoionization cross sections and polarizabilities. This method was extended in 1982 by Scott and Taylor [27] to exploit model potentials and to allow for relativistic effects by including terms from the Breit–Pauli Hamiltonian. A non-exchange version of the non-relativistic method was subsequently published by Burke and Scott [28]. In 1995, an updated version of the general method, to calculate electron–atom and electron–ion collision processes,with options to calculate radiative data and photoionization in either LS-coupling or in an intermediate-coupling scheme, was published by Berrington, Eissner and Norrington [29]. This method was based on two earlier methods [26,27] and included extensions by the Opacity Project [30,31] and the Iron Project team [32]. Zatsarinny [4] published a novel implementation of the R-matrix method with two significant innovations compared to the existing methods: non-orthogonal orbitals are used to represent both the bound and continuum one-electron orbitals; and a set of B-splines are used to define the R-matrix basis functions. The above mentioned methods are primarily concerned with low-energy scattering where the incident energy is insufficient to ionize the target. At intermediate energies, from close to the ionization threshold to several times this energy, modelling of the scattering processes is difficult because account must be taken of the coupling amongst the infinite number of continuum states of the ionized target and the infinite number of target bound states lying below the ionization threshold.

In this paper, we consider the photoionization and e-ion recombination of N^{+1} and Al^{+3} ions in the resonance energy region using a relativistic R-matrix method. The R-matrix method for electron—atom and photon—atom interactions has been discussed in great detail by Burke et. al.[33].The present calculations have been carried out by using the fully relativistic R-matrix code DARC [34-35].Where the detailed information about DARC [34-35] has been included in the package of the code[36].

In sec.2 ,the theory used in this paper will be introduced , in which the relativistic R-matrix method used to achieve the calculations for present paper ,where the relativistic atomic structure program GRASP is used to obtain bound orbitals from which the target ions are constructed in DARC code. Sec.3, deals with the results obtained by using this method,where the calculations have been performed on N^{+1}

ion in sec.3.1 and on Al^{+3} ion in sec.3.2,where the results obtained include the energy of levels ,the oscillator strength (f_{ij}) , radiative rates (A_{ji}) for an electric dipole allowed transitions ,line strength (S_{ij}), photoionization cross sections, photo-recombination cross sections and recombination rates ,while the conclusions are given in sec.4 .

2.Theory

The R-matrix method proceeds by partitioning configuration space into two regions by a sphere of radius $r = a$, where r is the relative coordinate of the scattering electron and the Centre of gravity of the target atom or ion. This sphere is chosen to completely envelope the electronic orbitals of the target atom or ion. Hence, in the internal region ($r \leq a$) exchange and correlation effects between the scattering electron and the target electrons must be included, whereas in the external region ($r > a$) exchange effects can be neglected and the problem simplifies considerably.

In this method , in the internal region, the 'target' or the 'core' ion is represented by an N-electron system interacting with the (N+1)th electron.The(N+1)th electron may be bound or in the continuum depending on its negative or positive energy (E). A coupled state of the (N +1)-electron system is made from a target state $\Phi = |J^t M^t\rangle$ and a single electron state $\phi = |jm\rangle$ as [36]:

$$A[\Phi,\phi]^{J,M} = \sum_{i=1}^{N+1} \frac{(-1)^{N+1-i}}{\sqrt{N+1}} [\Phi(r_1,\dots,r_{i-1},\dots,r_{i+1},\dots,r_{N+1}),\phi(r_i)]^{J,M}$$
$$= A \sum C(J^t jJ; M^t mM)|J^t M^t\rangle|jm\rangle \quad (1)$$

So A is an asymmetrisation operator to account for electron exchange which ensures that each term is antisymmetric with respect to interchange of the space and spin coordinates of any pair of the N + 1 electrons.The function Φ is the channel function represents the target state coupled with the spin and angular functions for the scattering electron , ϕ is the continuum basis orbitals for the scattered electron, i.e. the (N + 1)th electron function. Capture states are defined when all N + 1 single particle states are bound,$\theta = A[\Phi,\underline{\phi}]^{J,M}$, and are needed to make the wave function complete. All allowed coupled states for a total angular momentum J and parity π form the basis set Θ_k . The J and M superscripts are omitted from later equations. By the diagonalizing the (N+1)-Hamiltonian matrix $\langle\Theta_k|H^{N+1}|\Theta_{k'}\rangle$ over the internal region an orthonormal set of wavefunctions is obtained that can be written as [36]:

$$\Psi_k = \sum_{ij} c_{ijk}\, A[\Phi_i,\phi_{ij}] + \sum_m d_{mk}\theta_m \quad (2)$$

with eigenvalue E_k^{N+1} and eigenvector (c_{ijk}, d_{mk}) . The coefficients c_{ijk} and $d_{mk}$are determined by diagonalizing the total Hamiltonian of the whole system with the basis set expansion defined by eq.(2). Where k is the eigenvector index, j the continuum basis function index for a particular κ value, and i the channel index indicating a pair ($J^t\pi^t,\kappa$) coupled to get the total angular momentum J and parity π .The θ_m are bound channel functions of the (N+1)-electrons system that account for short range correlation and the orthogonality between the continuum and the bound electron orbitals i.e. scattered and target electrons.Note that for the continuum functions the radial integrals are over a finite range of integration even though the bra and ket notation is being used.

The total wavefunction which satisfies the time-independent Dirac equation [36]:

$$H^{N+1}\,\Psi = E\Psi \quad (3)$$

for any energy E is expanded in terms of the basis of eq.(2) as [36] :

$$\Psi_E = \sum_k A_{Ek}\Psi_k \quad (4)$$

The relativistic Dirac Hamiltonian in the Dirac R-matrix method for (N+1) electron target atoms or ions with nuclear charge number Z is given in atomic units by [36]:

$$H^{N+1} = \sum_{i=1}^{M+1}(-ic\alpha.\nabla_i + (\beta-1)c^2 + V(r_i)) + \sum_{j=i+1}^{M+1}\frac{1}{|r_j - r_i|} \quad , \quad (5)$$

where i and j index the individual electrons,the electron rest mass has been subtracted, and α and β are 4×4-dimensional Dirac matrices constructed from Pauli spin and unit matrices defined by [36] :

$$\alpha = \begin{pmatrix} 0 & \sigma \\ \sigma & 0 \end{pmatrix} \ , \ \beta = \begin{pmatrix} I_2 & 0 \\ 0 & -I_2 \end{pmatrix} \quad (6)$$

where the components of σ , σ_x , σ_y and σ_z are 2×2 Pauli spin matrices defined by :

$$\sigma_x = \begin{pmatrix} 0 & 1 \\ 1 & 0 \end{pmatrix} \ , \quad \sigma_y = \begin{pmatrix} 0 & -i \\ i & 0 \end{pmatrix} \ , \quad \sigma_z = \begin{pmatrix} 1 & 0 \\ 0 & -1 \end{pmatrix} \quad (7)$$

and I_2 and I_4 are 2×2 and 4×4 unit matrices, respectively. The first three one-electron terms in the Dirac Hamiltonian are a momentum term, mass term and the electron-nucleus Coulomb attraction. The final two-electron term is the Coulomb electron-electron repulsion. The Hamiltonian matrix element can be split so that angular integrals are calculated using Racah algebra and radial integrals by numerical quadrature. Further relativistic corrections, for example the Breit interaction (a virtual photon exchanged between electrons) and other quantum electrodynamic (QED) corrections, self-energy and vacuum polarisation, are not included in the Hamiltonian. However, the eigenvalues of the Hamiltonian may be adjusted to approximate these effects and providing the changes are small.This appears to be a reasonable approach [36].

With large complex systems the computational problem can be drastically reduced by using a model potential to describe the inner closed shell core of electrons. Integrals then only need to be calculated for valence electrons, which form excited states, and continuum electrons. where there are M valence electrons in the target and $V(r)$ is the model potential satisfying the boundary conditions [36]:

$$V(r) \sim -\frac{Z}{r} \ \ when \ r \to 0 \ , \ V(r) \sim -\frac{Z-N}{r} \ \ when \ r \to \infty \quad , \quad (8)$$

Although the basis that will be constructed from one-electron orbitals is reduced in size,the continuum functions have to be orthogonalised with the full set of bound orbitals.

Target N-electron states are labelled by total angular momentum J^t and parity π^t. These states are constructed from linear combinations of configuration state functions (CSFs) which have the same angular momentum and parity.Thus a target state, or level, can be distinguished by the CSF mixing coefficients and it has a particular energy. The (N+1)-electron, or target+electron, system is also characterised by total angular momentum J and overall parity π . J is formed by coupling vectorially J^t and j , the total angular momentum of the additional electron. The possible ways of doing this are governed by the triangular relation $|J^t - j| \leq J \leq J^t + j$, where the minimum difference between each J is 1. Then each pair $J\pi$ are referred to as a "symmetry".Also the (N + 1)th electron is labelled by quantum number κ which is equivalent to specifying both j and the orbital angular momentum l .$(2j + 1 = 2|\kappa|, if\ k < 0\ then\ l =$

$-\kappa \; else \; \kappa > 0 \; and \; l = \kappa$). Thus a symmetry of the (N + 1)-system is composed of the possible "channels" which are labelled by $(J^t\pi^t, \kappa)$ pairs , so the angular momentum and parity will be conserved. In a scattering process the symmetry will be conserved. The channel will not change for elastic scattering but will for inelastic scattering. It may take the sum of many symmetries for a calculation to converge as the scattering energy increases and with it the number of energetically accessible channels. This corresponds to the familiar partial wave expansion in low energy potential scattering. In photoionization the symmetry is not conserved. The electric dipole transition process involves absorption of a photon with angular momentum 1 and a change of parity. Therefore photoionization

$$\frac{Q_i(a)}{\mathcal{P}_i(a)} = \frac{b+\kappa}{2ac}$$

for all i , where $P_i(a)$ and $Q_i(a)$ are the large and small radial component of the continuum electron at the boundary, respectively, and b is an arbitrary constant.

$$\frac{d\mathcal{P}_i}{dr}|_{r=a} = \frac{b}{a}\mathcal{P}_i(a) \qquad (10)$$

Then using the Hamiltonian eq.(5) and the boundary conditions eq.(9), an expression for the expansion coefficients is found as [38]:

$$A_{Ek} = \frac{1}{2a(E_k^{N+1} - E)} \sum_i w_{ik}(a)[2ac\, Q_i(a) - (b+\kappa_i)\, P_i(a)] \qquad (11)$$

Where $w_{ik}(a)$ surface amplitudes at the boundary $r = a$. Substitution of $\Psi_E(e + ion)$ expansion in the Dirac equation ,eq.(3) results a set of coupled equations that are solved using the R-matrix method. The solution is a continuum wave function, Ψ_{fE}^- for an electron at positive energies ($E > 0$) , or a bound state, Ψ_i , at a negative total energy ($E \leq 0$). The complex resonant structures in photoionization and recombination result from channel couplings between continuum channels that are open ($k_i^2 > 0$), and ones that are closed ($k_i^2 < 0$), at electron energies k_i^2 corresponding to the Rydberg series converging on to the target thresholds.

from a particular bound state restricts the number of symmetries in the calculation to two or three.On the other hand , the energy will be also conserved ,where if E^{N+1} is the total energy of the electronic system and E_i^N the energy of the target state coupled to the *i* th channel then the channel energy of a scattered electron is $\in_i = E^{N+1} - E_i^N$. An open channel has $\in_i > 0$, a closed channel has $\in_i < 0$ and at the channel threshold $\in_i = 0$. For photoionisation by a photon with incident energy ω of an atom in an initial bound state with energy E_0^{N+1} the channel energy is similarly $\in_i = \omega + E_0^{N+1} - E_i^N$ .Where all channels are closed in a bound state [36]. Then the boundary condition at r = a is chosen as [36]:

(9)

The boundary condition reduces in the nonrelativistic limit ($c \to \infty \; or \; \alpha \to 0$) to that of burke et.al. [37]:

Transition matrix elements for photoionization or electron–ion recombination can be obtained using the bound and continuum wave functions as $|\langle \Psi_B || D_1 || \Psi_F \rangle| = \langle \Psi_{jE}^-(\bar{\boldsymbol{k}}) || D_1 || \Psi_i \rangle$, D_1 is either the dipole length operator or the dipole velocity operator where $D_1^L = \sum_{l=1}^{N+1} r_l$ is the dipole length operator, and $D_1^V = \sum_{l=1}^{N+1} c\, \boldsymbol{\alpha}_l$ is the dipole velocity operator , the sum represents the number of electrons. The transition matrix elements sometimes called reduced dipole matrix elements can be reduced to generalized line strength as [39]:

$S = \sum_{ljJ} |\langle \Psi_{jE}^{-} || D_1 || \Psi_i \rangle|^2$ (12)

Where S related with the reduced dipole matrix elements ,defined in either length form S_L or velocity form S_V ,by the equations (in atomic units) [39]:

$$S_L = \sum_{ljJ} \left| < \Psi_{jE}^{-} | \sum_{j=1}^{N+1} r_j | \Psi_i > \right|^2 \quad (13)$$

$$S_V = \omega^{-2} \sum_{ljJ} \left| < \Psi_{jE}^{-} | \sum_{j=1}^{N+1} \nabla_j | \Psi_i > \right|^2 \quad (14)$$

Where Ψ_i and Ψ_{jE}^{-} are the initial bound state and final continuum state wave functions, respectively.

Dipole transition oscillator strengths $f(b,a)$, and thus transition rates, can be calculated like photoionization cross sections using two R-matrix bound states [36] :

$$f(b,a) = \frac{2C}{3g_a} |\langle \Psi_a || D_1 || \Psi_b \rangle|^2 \quad (15)$$

Where $g_a = 2J_a + 1$ is the statistical weight of the initial state a in jj-coupling. $C = w$ in the length form and $C = w^{-1}$ in the velocity form.

The photoionization cross section is proportional to the generalized line strength in length and velocity forms by equations in atomic units [39]:

$$\sigma_{ij}^{L,V} = \frac{8\pi^2 \alpha\, \omega}{3g_i} S_{L,V} \quad (16)$$

Where g_i is the statistical weight factor of the bound state and ω is the incident photon energy.

Recombination cross sections can be obtained in length and velocity forms $\sigma_{RC}^{L,V}$ by using the principle of detailed balance or Milne relation as [39]:

$$\sigma_{RC}^{L,V} = \sigma_{ij}^{L,V} \frac{g_i}{g_j} \frac{h^2\omega^2}{4\pi^2 m^2 c^2 v^2} \quad (17)$$

Where g_j is the statistical weight factor of the recombined state and v is the photoelectron velocity.

The radiative decay rate (Einstein's A-coefficient) given by [40] :

$$A_{ji}(a.u.) = \frac{1}{2}\alpha^3 \frac{g_i}{g_j} E_{ji}^2 f(b,a) \quad (18)$$

Where E_{ji} is the energy difference between the initial and final states,

$$A_{ji}(sec^{-1}) = \frac{A_{ji}(a.u.)}{\tau_o} \quad (19)$$

where α is the fine-structure constant and $\tau_o = 2.4191 \times 10^{-17} sec$ is the atomic unit of time [40].

The unified total recombination rate coefficient (recombination rates) is given by [41]:

$$\alpha_{RC}(E) = v\sigma_{RC}(E) \quad (20)$$

Where v is the photoelectron velocity. $\alpha_{RC}(E)$ reveals detailed resonant features in electron–ion recombination spectrum and is of considerable interest to experimental facilities.

3. Calculations

The energy of levels ,the oscillator strength (f_{ij}) , radiative rates (A_{ji}) for an electric dipole allowed transitions ,line strength (S_{ij}), photoionization cross sections $\sigma_{RC}^{L,V}$, photo-recombination cross sections $\sigma_{RC}^{L,V}$ and recombination rates $\alpha_{RC}(E)$ of N^{+1} and Al^{+3} ions are investigated and calculated using the fully relativistic R-matrix method.A relativistic atomic structure program GRASP is used to obtain bound orbitals from which the target ions are constructed in DARC. Where the calculations are carried out with determination of target wave function. The wave function have been obtained by using the GRASP code ,The present calculations have been carried out by using the relativistic R-matrix code DARC [34,35].The author of the DARC code is preparing a manual to be published and he suggested that the above references for the DARC. However, the detailed information has been included in the package of the code[36].The Dirac R-matrix theory is based on the Dirac atomic structure code known as GRASP ,where GRASP is an acronym for the General-purpose Relativistic Atomic Structure Program developed by Grant et. al. ,the version of GRASP is included as a DARC module where adopted in present calculations [36]. This is a fully relativistic code, and is based on the *jj* coupling scheme. Additionally, the option of extended average level (EAL) are used , in which a weighted (proportional to $2j+1$) trace of the Hamiltonian matrix is minimized. This produces a compromise set of orbitals describing closely lying states with good accuracy [42].

3.1 N^{+1} ion

N^{+1} ion has a simple atomic structure where the wave function for target or core ion N^{+2} includes the state $n=1$ and $n=2$. The configuration for target or core ion N^{+2} is $(1s^2 2s^1 2p^2, 1s^1 2s^2 2p^2, 1s^2 2s^0 2p^3, 1s^2 2s^2 2p^0)$ this configuration gives rise to 23 fine-structure levels of N^{+2}, as given in table (1). The Dirac wave functions of the bound orbitals for the N^{+2} ion (someties is refer to as N III) have been calculated using GRASP code [36],to give a number of continuum basis functions helped to solve the dipole matrix elements of DARC [34,35].The initial ground state of N^{+1} ion has total $J=0$ and even parity. The final state of the $N^{+2}+e^-$ system has total $J=1$ and odd parity. The configurations of the core ion in the relativistic calculation are formed from Dirac-Hartree-Fock orbitals from a GRASP EAL calculation with 23 relativistic configurations.

Table (1) shows the energies of the levels of the target ion N^{+2} in the eigen function expansion of N^{+1} ion for the GRASP EAL ,with QED plus Breit corrections, where the quantum electro-dynamic QED with Breit corrections are not included in the GRASP energies, which are considered as zero-order energies , also the DARC calculation which is using the Dirac orbitals and the results obtained from the atomic structure code AUTOSTRUCTURE[43].The results from GRASP , DARC and AUTOSTRUCTURE[43] are in good agreement .

Table (1) : Ground state energy and excitation energies in rydberg for N^{+2} with QED plus Breit correction from GRASP compare with DARC and AUTOSTRUCTURE[43].

Index	Term	Parity	J	GRASP	Breit + QED	DARC	A.S.
1	$1s^2 2s^2 2\bar{p}^1$(2P)	O	1/2	-.105745154E+03	.14940E-01	-.105745100E+03	-.105528304E+03
2	$1s^2 2s^2 2p^1$(2P)	O	3/2	.171459765E-02	-.29981E-03	.170261579E-02	.188719000E-02
3	$1s^2 2s^1 2p^2$(4P)	E	1/2	.457098055E+00	-.16410E-03	.457076360E+00	.496830890E+00
4	$1s^2 2s^1 2p^2$(4P)	E	3/2	.457679479E+00	-.25800E-03	.457653570E+00	.497487430E+00
5	$1s^2 2s^1 2p^2$(4P)	E	5/2	.458645107E+00	-.60500E-03	.458612235E+00	.498575630E+00
6	$1s^2 2s^1 2\bar{p}^1 2p^1$(2D)	E	3/2	.976328031E+00	-.38300E-03	.976299377E+00	.948679270E+00
7	$1s^2 2s^1 2\bar{p}^1 2p^1$(2D)	E	5/2	.976342708E+00	-.48200E-03	.976314021E+00	.948682510E+00
8	$1s^2 2s^1 2\bar{p}^2$(2S)	E	1/2	.125659906E+01	-.19420E-03	.125657035E+01	.118416225E+01
9	$1s^2 2s^1 2\bar{p}^1 2p^1$(2P)	E	1/2	.144961275E+01	-.18330E-03	.144958987E+01	.137738008E+01
10	$1s^2 2s^1 2\bar{p}^1 2p^1$(2P)	E	3/2	.145076443E+01	-.48200E-03	.145073323E+01	.137868342E+01
11	$1s^2 2p^3$(4S)	O	3/2	.166685165E+01	-.60600E-03	.166680067E+01	.168938208E+01
12	$1s^2 2\bar{p}^1 2p^2$(2D)	O	3/2	.194711202E+01	-.53300E-03	.194706101E+01	.192486115E+01
13	$1s^2 2\bar{p}^1 2p^2$(2D)	O	5/2	.194711910E+01	-.75100E-03	.194706802E+01	.192486973E+01
14	$1s^2 2\bar{p}^1 2p^2$(2P)	O	1/2	.223657499E+01	-.40900E-03	.223652615E+01	.216324390E+01
15	$1s^2 2\bar{p}^2 2p^1$(2P)	O	3/2	.223667612E+01	-.46700E-03	.223662660E+01	.216332984E+01
16	$1s^1 2s^2 2p^2$(4P)	E	1/2	.297534985E+02	-.10440E-01	.297535051E+02	.306505891E+02
17	$1s^1 2s^2 2p^2$(4P)	E	3/2	.297545845E+02	-.10410E-01	.297545869E+02	.306512464E+02
18	$1s^1 2s^2 2p^2$(4P)	E	5/2	.297563771E+02	-.11180E-01	.297563725E+02	.306523339E+02
19	$1s^1 2s^2 2\bar{p}^1 2p^1$(2D)	E	3/2	.300385176E+02	-.10360E-01	.300385177E+02	.308572182E+02
20	$1s^1 2s^2 2\bar{p}^1 2p^1$(2D)	E	5/2	.300388209E+02	-.11530E-01	.300388195E+02	.308584925E+02
21	$1s^1 2s^2 2\bar{p}^1 2p^1$(2P)	E	1/2	.300457421E+02	-.11450E-01	.300457447E+02	.308771538E+02
22	$1s^1 2s^2 2\bar{p}^1 2p^1$(2P)	E	3/2	.300480499E+02	-.11400E-01	.300480426E+02	.308771889E+02
23	$1s^1 2s^2 2\bar{p}^2$(2S)	E	1/2	.303190607E+02	-.10810E-01	.303190591E+02	.311126436E+02

The absorption oscillator strength f_{ij} and radiative rate A_{ji} for an allowed transition $i \to j$ are related by eq.(18), and S is the line strength.Table (2) gives present transition energies ΔE_{ij}(Ang.), oscillator strengths f_{ij} , radiative rate $A_{ji}(\sec^{-1})$ and line-strength S_{ji} (a.u.) obtained from GRASP in length form only, for the 95 electric dipole (E1) allowed transitions among the 23 levels of N^{+2}. The present results are compared with the results obtained by using the atomic structure code AUTOSTRUCTURE[43] where the AUTOSTRUCTURE[43] results obtained by using the theoretical transition energies and the same configurations for target or core ion N^{+2} that were employed to determine the energies for AUTOSTRUCTURE[43] as listed in table (1). The present results obtained by using the fully relativistic GRASP code[36],Some of the AUTOSTRUCTURE [43] results agree well with the GRASP calculations, but for other transitions, they have the same behavior with transition energy ,so the results are in satisfactory agreement.The indices used to represent the lower and upper levels of a transition have been defined in table (1). While calculating the oscillator strengths and radiative rates, the quantum electro-dynamic QED plus Breit corrected energies are used in the calculations as listed in table (1).

Table (2) : Transition energies ΔE_{ij}(Ang.), radiative rates A_{ji}($\sec^{-1}$) ,oscillator strengths f_{ij} and line-strength S_{ji}(a.u.) of N^{+2} obtained from GRASP are compared with the results obtained by using the atomic structure code AUTOSTRUCTURE[43].

		GRASP				A.S.		
i	j	ΔE_{ij}	A_{ji}	f_{ij}	S_{ji}	A_{ji}	f_{ij}	S_{ji}
1	3	.1041E+03	.1210E+03	.7217E-07	.9477E-06	.7103E+03	.3583E-06	.4000E-05
1	4	.1042E+03	.3133E+01	.3729E-08	.4891E-07	.1748E+02	.1759E-07	.0000E+00
1	6	.2223E+03	.5602E+09	.1465E+00	.9004E+00	.7278E+09	.2014E+00	.1273E+01
1	8	.2862E+03	.1161E+10	.9157E-01	.4373E+00	.1270E+10	.1128E+00	.5713E+00
1	9	.3302E+03	.4362E+10	.2585E+00	.1070E+01	.5288E+10	.3471E+00	.1512E+01
1	10	.3304E+03	.1094E+10	.1295E+00	.5359E+00	.1328E+10	.1739E+00	.7571E+00
1	16	.6776E+04	.1857E+08	.2613E-05	.5271E-06	.5609E+07	.7430E-06	.0000E+00
1	17	.6777E+04	.1522E+07	.4283E-06	.8639E-07	.1598E+05	.4236E-08	.0000E+00
1	19	.6841E+04	.5657E+12	.1562E+00	.3121E-01	.7936E+12	.1038E+00	.2018E-01
1	22	.6843E+04	.1831E+12	.5053E-01	.1009E-01	.2813E+12	.7345E-01	.1428E-01
1	23	.6905E+04	.1801E+12	.2441E-01	.4831E-02	.1031E+12	.1326E-01	.2557E-02
2	3	.1038E+03	.1498E+03	.4494E-07	.1184E-05	.7685E+03	.3906E-06	.5000E-05
2	4	.1039E+03	.1177E+02	.7046E-08	.1854E-06	.1328E+03	.1347E-06	.2000E-05
2	5	.1040E+03	.8006E+02	.7170E-07	.1884E-05	.4396E+03	.6655E-06	.8000E-05
2	6	.2220E+03	.1103E+09	.1446E-01	.1780E+00	.1422E+09	.3949E-01	.2502E+00
2	7	.2220E+03	.6672E+09	.1312E+00	.1616E+01	.8652E+09	.3604E+00	.2284E+01
2	8	.2859E+03	.2273E+10	.8983E-01	.8589E+00	.2461E+10	.2192E+00	.1112E+01
2	9	.3299E+03	.2206E+10	.6549E-01	.5427E+00	.2684E+10	.1767E+00	.7705E+00
2	10	.3301E+03	.5476E+10	.3248E+00	.2690E+01	.6652E+10	.8740E+00	.3808E+01
2	16	.6776E+04	.1697E+07	.1194E-06	.4817E-07	.2612E+06	.3463E-07	.0000E+00
2	17	.6776E+04	.2533E+08	.3564E-05	.1438E-05	.7468E+07	.1979E-05	.0000E+00
2	18	.6776E+04	.1869E+08	.3946E-05	.1592E-05	.6126E+07	.2435E-05	.0000E+00
2	19	.6841E+04	.1038E+11	.1434E-02	.5730E-03	.3932E+12	.5140E-01	.9998E-02
2	20	.6841E+04	.5450E+12	.1129E+00	.4512E-01	.9649E+12	.2524E+00	.4907E-01
2	21	.6842E+04	.5850E+12	.4037E-01	.1613E-01	.3644E+12	.1427E+00	.2774E-01
2	22	.6843E+04	.1556E+13	.2148E+00	.8580E-01	.8479E+11	.2215E-01	.4304E-02
2	23	.6905E+04	.3765E+12	.2552E-01	.1010E-01	.2135E+12	.2746E-01	.5295E-02
3	11	.2755E+03	.9369E+09	.1595E+00	.7914E+00	.1209E+10	.2117E+00	.1065E+01
3	12	.3394E+03	.1908E+03	.2141E-07	.8624E-07	.6041E+03	.7375E-07	.0000E+00
3	14	.4054E+03	.4231E+04	.1664E-06	.5610E-06	.7561E+04	.3390E-06	.1000E-05
3	15	.4054E+03	.4715E+02	.3708E-08	.1250E-07	.2172E+03	.1948E-07	.0000E+00
4	11	.2754E+03	.1871E+10	.1594E+00	.1582E+01	.2414E+10	.4230E+00	.2130E+01
4	12	.3393E+03	.3383E+04	.1899E-06	.1530E-05	.6716E+04	.8205E-06	.3000E-05
4	13	.3392E+03	.3913E+03	.3296E-07	.2657E-06	.7040E+03	.1291E-06	.1000E-05
4	14	.4052E+03	.4413E+03	.8683E-08	.5858E-07	.1441E+04	.6465E-07	.0000E+00
4	15	.4053E+03	.6474E+04	.2547E-06	.1718E-05	.1731E+05	.1553E-05	.6000E-05
5	11	.2753E+03	.2801E+10	.1593E+00	.2373E+01	.3611E+10	.6340E+00	.3194E+01
5	12	.3391E+03	.6887E+03	.2580E-07	.3119E-06	.2448E+04	.2997E-06	.1000E-05
5	13	.3391E+03	.1175E+05	.6604E-06	.7987E-05	.2443E+05	.4485E-05	.1900E-04
5	15	.4051E+03	.1768E+04	.4640E-07	.4697E-06	.7739E+04	.6955E-06	.3000E-05
6	11	.1573E+03	.2505E+00	.6545E-10	.1138E-08	.1715E+02	.7785E-08	.0000E+00
6	12	.2211E+03	.1303E+10	.1722E+00	.2129E+01	.1780E+10	.4652E+00	.2859E+01
6	13	.2211E+03	.9793E+08	.1942E-01	.2401E+00	.1346E+09	.5275E-01	.3244E+00
6	14	.2871E+03	.2900E+10	.1137E+00	.1082E+01	.3367E+10	.2842E+00	.1404E+01
6	15	.2871E+03	.2929E+09	.2296E-01	.2186E+00	.3438E+09	.5800E-01	.2866E+00
7	11	.1573E+03	.1157E+02	.2015E-08	.5253E-07	.2020E+03	.9165E-07	.1000E-05
7	12	.2212E+03	.1481E+09	.1304E-01	.2418E+00	.2059E+09	.5380E-01	.3306E+00
7	13	.2211E+03	.1355E+10	.1791E+00	.3323E+01	.1857E+10	.7275E+00	.4473E+01
7	15	.2871E+03	.2599E+10	.1358E+00	.1939E+01	.3010E+10	.5080E+00	.2509E+01
8	11	.9337E+02	.1076E-01	.1595E-10	.2335E-09	.8080E+01	.7880E-08	.0000E+00
8	12	.1572E+03	.1582E+05	.8270E-05	.7190E-04	.6061E+05	.2751E-04	.2230E-03
8	14	.2232E+03	.4451E+09	.5773E-01	.3535E+00	.6221E+09	.8080E-01	.4951E+00
8	15	.2232E+03	.4557E+09	.1182E+00	.7238E+00	.6410E+09	.1665E+00	.1020E+01
9	11	.4940E+02	.9787E+01	.5184E-07	.1435E-05	.1050E+03	.2686E-06	.5000E-05
9	12	.1133E+03	.1633E+09	.1645E+00	.1986E+01	.2945E+09	.2446E+00	.2681E+01
9	14	.1792E+03	.8479E+09	.1706E+00	.1301E+01	.1098E+10	.2213E+00	.1690E+01
9	15	.1793E+03	.2068E+09	.8319E-01	.6344E+00	.2639E+09	.1064E+00	.8120E+00
10	11	.4920E+02	.3419E+02	.9126E-07	.5071E-05	.5064E+03	.1306E-05	.2500E-04
10	12	.1131E+03	.3193E+08	.1614E-01	.3902E+00	.5661E+08	.4725E-01	.5190E+00
10	13	.1130E+03	.1938E+09	.1470E+00	.3557E+01	.3481E+09	.4359E+00	.4788E+01

10	14	.1790E+03	.4194E+09	.4227E-01	.6454E+00	.5401E+09	.1093E+00	.8355E+00
10	15	.1791E+03	.1056E+10	.2128E+00	.3249E+01	.1365E+10	.5520E+00	.4222E+01
11	16	.6397E+04	.4312E+09	.3405E-04	.1455E-04	.1397E+11	.2074E-02	.4300E-03
11	17	.6397E+04	.4314E+09	.6812E-04	.2911E-04	.1397E+11	.4148E-02	.8590E-03
11	18	.6397E+04	.4312E+09	.1021E-03	.4364E-04	.1398E+11	.6220E-02	.1289E-02
11	19	.6462E+04	.1733E+04	.2682E-09	.1135E-09	.1780E+06	.2604E-07	.0000E+00
11	20	.6461E+04	.1824E+06	.4235E-07	.1792E-07	.4285E+06	.1254E-06	.0000E+00
11	21	.6463E+04	.1520E+06	.1175E-07	.4972E-08	.4422E+06	.1939E-06	.0000E+00
11	22	.6464E+04	.4085E+06	.6319E-07	.2673E-07	.9098E+05	.2659E-07	.0000E+00
11	23	.6525E+04	.2770E+05	.2102E-08	.8807E-09	.5646E+05	.8120E-08	.0000E+00
12	16	.6333E+04	.1085E+05	.8739E-09	.3773E-09	.3238E+05	.4886E-08	.0000E+00
12	17	.6333E+04	.2132E+04	.3434E-09	.1483E-09	.8615E+05	.2599E-07	.0000E+00
12	18	.6333E+04	.4502E+01	.1088E-11	.4696E-12	.1672E+05	.7570E-08	.0000E+00
12	19	.6398E+04	.6018E+08	.9500E-05	.4060E-05	.1460E+11	.2171E-02	.4500E-03
12	20	.6398E+04	.8545E+06	.2024E-06	.8648E-07	.1122E+10	.3337E-03	.6900E-04
12	21	.6399E+04	.2050E+10	.1617E-03	.6909E-04	.1075E+10	.4790E-03	.9900E-04
12	22	.6400E+04	.1429E+09	.2255E-04	.9633E-05	.1519E+11	.4512E-02	.9350E-03
12	23	.6462E+04	.5165E+06	.3997E-07	.1691E-07	.6316E+06	.9230E-07	.0000E+00
13	17	.6333E+04	.3510E+05	.3770E-08	.2441E-08	.3971E+05	.1198E-07	.0000E+00
13	18	.6333E+04	.2155E+03	.3472E-10	.2248E-10	.2524E+06	.1142E-06	.0000E+00
13	20	.6398E+04	.3101E+08	.4896E-05	.3139E-05	.1363E+11	.4054E-02	.8410E-03
13	22	.6400E+04	.1766E+10	.1857E-03	.1190E-03	.1242E+10	.3691E-03	.7600E-04
14	16	.6267E+04	.8140E+06	.1339E-06	.2921E-07	.3388E+06	.5200E-07	.0000E+00
14	17	.6267E+04	.9448E+05	.3109E-07	.6781E-08	.2000E+04	.6135E-09	.0000E+00
14	19	.6332E+04	.2137E+11	.6887E-02	.1487E-02	.6576E+10	.9945E-03	.2080E-03
14	22	.6334E+04	.9625E+10	.3101E-02	.6692E-03	.7789E+09	.2352E-03	.4900E-04
14	23	.6396E+04	.7530E+10	.1190E-02	.2543E-03	.2083E+11	.3095E-02	.6410E-03
15	16	.6267E+04	.2654E+05	.2184E-08	.9527E-09	.6463E+05	.9915E-08	.0000E+00
15	17	.6267E+04	.1345E+07	.2213E-06	.9655E-07	.2941E+06	.9025E-07	.0000E+00
15	18	.6267E+04	.7671E+06	.1893E-06	.8257E-07	.1990E+06	.9160E-07	.0000E+00
15	19	.6332E+04	.1797E+09	.2897E-04	.1251E-04	.3237E+10	.4894E-03	.1020E-03
15	20	.6332E+04	.1987E+11	.4804E-02	.2074E-02	.7968E+10	.2410E-02	.5040E-03
15	21	.6333E+04	.2871E+11	.2312E-02	.9983E-03	.1082E+10	.4899E-03	.1020E-03
15	22	.6334E+04	.7564E+11	.1219E-01	.5259E-02	.2783E+09	.8405E-04	.1800E-04
15	23	.6396E+04	.1581E+11	.1249E-02	.5339E-03	.4198E+11	.6235E-02	.1293E-02

The number of continuum orbitals per angular momentum for the wave function of the target or core ion N^{+2} is equal to 18 , the R-matrix boundary equal to 6.00 a.u. and the arbitrary constant b of eq.(9) is zero. The calculated ionization energy for N^{+1} ion by DARC is 1.12587 a.u. compare with 1.19543 a.u. obtained from the atomic structure code AUTOSTRUCTURE[43].The total cross section leave the residual core ion in all accessible target states ,where it is of a given state corresponds to the sum of the partial photoionization cross sections in to the ground state as well as the excited states of the residual core ion.Figure (1) show the total photoionization cross section of N^{+1} ion in the length and velocity gauge obtained by eq.(16) in the photon energy rage of 2.0 to 5.0 rydberg which covers all the thresholds in the N^{+2} target states, and the resonances of the dominant Rydberg series can be seen clearly for the present results.The present results are compared with the theoretical results of Nahar and Pradhan[44],where the present length and velocity results are in good agreement with each other and with the results of Nahar and Pradhan[44] , and these results have the similar behavior with energy.This agreement is due to core excitations ,where they are formed due to doubly excited rydberg states converging to core thresholds.The resonance peak appear when the excitation threshold is approached and drop almost to minimum as photon energy is used for excitation and electron is released .In general the agreement is very good for the present calculations.

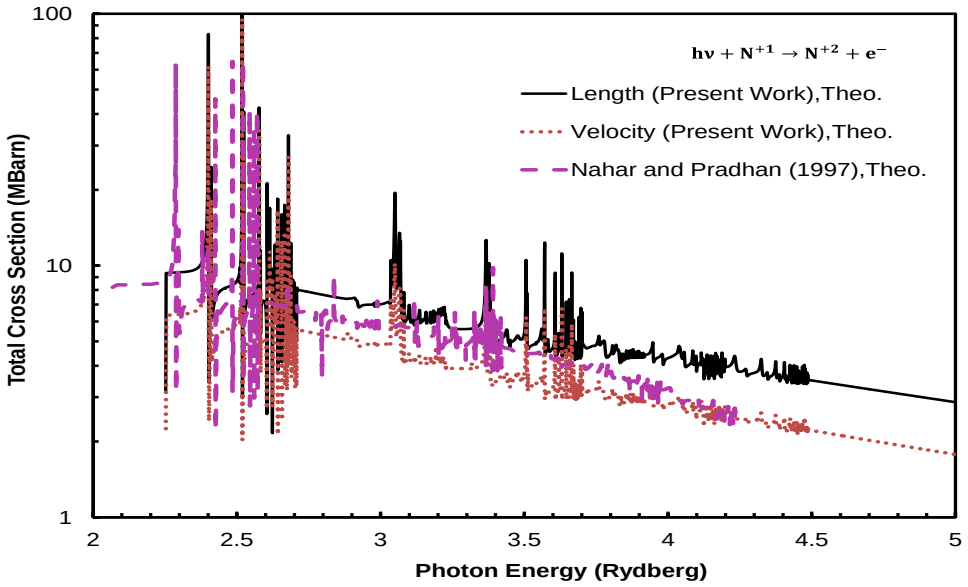

Figure (1) : Total photoionization cross section of N^{+1} ion in the length and velocity gauge using 23 target states .

According to the results of photoionization cross section of N^{+1} ion,the recombination cross sections , can be obtained in length and velocity forms $\sigma_{RC}^{L,V}$ by using eq.(17), according to the principle of detailed balance or Milne relation [39]. Figure (2) show the total recombination cross section of ($e^- + N^{+2} \rightarrow N^{+1} + h\nu$) processes in the photon energy range of 2.0 to 5.0 rydberg ,the comparison here made between length and velocity gage, the recombination cross section diverges at 2.25 rydberg of photon energy where this energy equal to ionization energy for N^{+1} ion, and then it decays with energy until resonance appear at increases energies. The resonance appear on to the $n = 1$ and $n = 2$ threshold of core N^{+2} ion , where the resonance represent the capture of electron,the resonance peak appear when the excitation threshold is approached and drop almost to minimum as photon energy is used for excitation and electron is released,these resonance complexes is according to core excitations,where they are formed according to doubly excited rydberg states converging to core thresholds [45]. In general the resonance can be observed in the recombination spectra as a peak lines .There is a good agreement for the present target states calculations between the length and velocity gage which covers the thresholds in the N^{+2} ion target states.

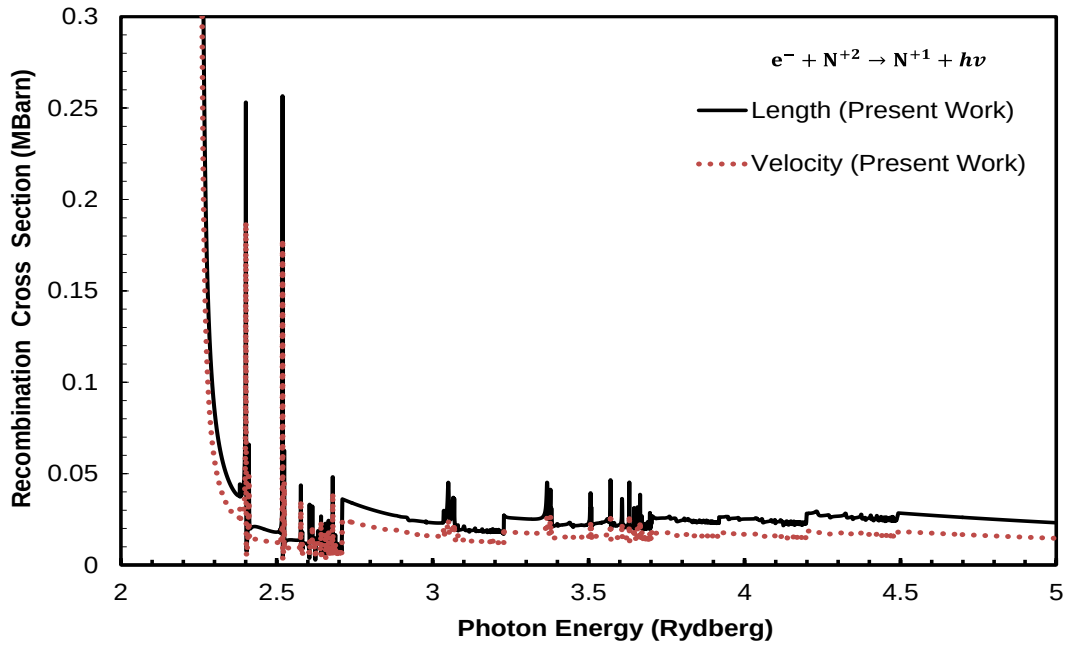

Figure (2) : Total recombination cross section of $(e^- + N^{+2} \rightarrow N^{+1} + h\nu)$ in the length and velocity gauge using 23 target states .

The total recombination cross-sections and the recombination rates are related to each other according eq.(20) through the velocity of photoelectron and hence show similar detailed resonant features. Figure (3) show the total photo-recombination rates of $(e^- + N^{+2} \rightarrow N^{+1} + h\nu)$ process in the photon energy range of 2.0 to 5.0 rydberg.The calculated rates show detailed resonant structures similar to that of figure (2),where the recombination rates diverges at 2.25 rydberg of photon energy. The resonance appear on to the $n = 1$ and $n = 2$ thresholds of the recombination rates and can be observed in the recombination rates spectra as peak lines as discussed in figure (2). There is a good agreement for the present target states calculations between the length and velocity gage which covers the thresholds in the N^{+2} ion target states.

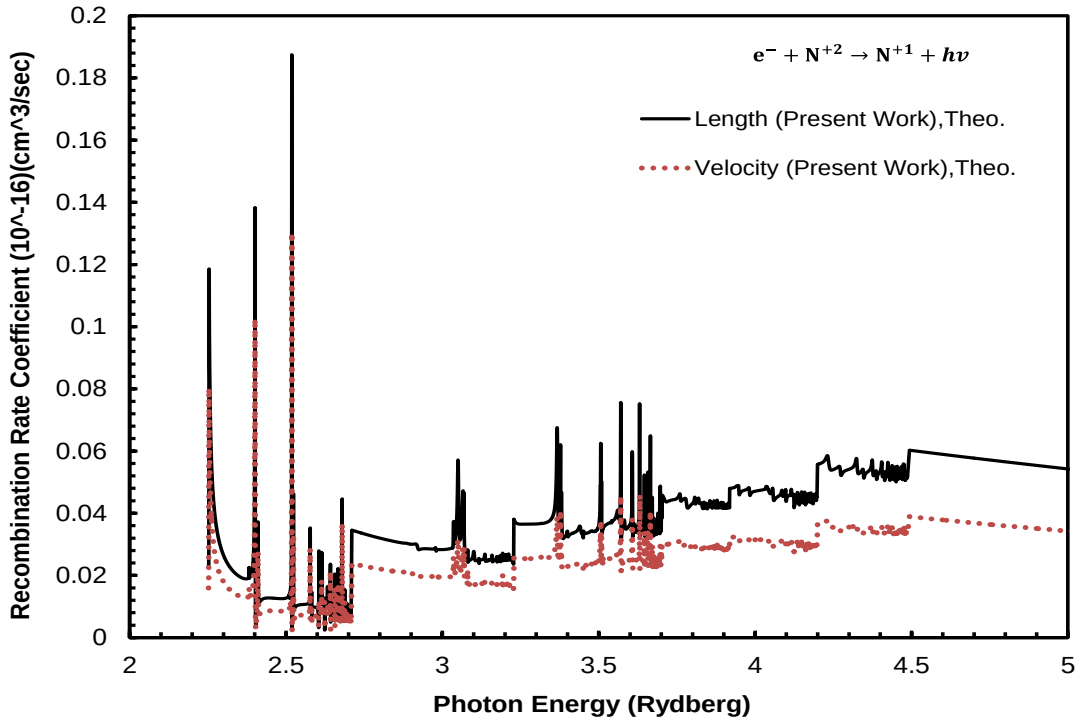

Figure (3) : Total recombination rates of $(e^- + N^{+2} \rightarrow N^{+1} + h\nu)$ in the length and velocity gauge using 23 target states .

3.2 Al^{+3} ion

The wave function for target or core ion Al^{+4} includes the core common to all CSFs which is $(1s^2)$,and consist of state $n = 1, 2$ and $n = 3$ with the configurations $(2s^2 2p^5, 2s^1 2p^6 \text{and } 2s^2 2p^4 3s^1)$, these configurations give rise to 11 fine-structure levels of Al^{+4} ion ,as given in table (5-8). The Dirac wave functions of the bound orbitals for the Al^{+4} ion have been calculated using GRASP code [36],to give a number of continuum basis functions helped to solve the dipole matrix elements of DARC [34,35].The initial ground state of Al^{+3} ion has total $J = 0$ and even parity. The final state of the $Al^{+4} + e^-$ system has total $J = 1$ and odd parity. The configurations of the core ion in the relativistic calculation are formed from Dirac-Hartree-Fock orbitals from a GRASP EAL calculation with 11 relativistic configurations.

Table (3) shows the energies of the levels of the target ion Al^{+4} in the eigen function expansion of Al^{+3} ion for the GRASP EAL ,with QED plus Breit corrections, where the QED with Breit corrections are not included in the GRASP energies, which are considered as zero-order energies , also the DARC calculation using the Dirac orbitals and the results obtained from the atomic structure code AUTOSTRUCTURE[43].The results obtained from GRASP , DARC and AUTOSTRUCTURE[43] are in good agreement .

Table (3) : Ground state energy and excitation energies in rydberg for Al^{+4} with QED plus Breit correction from GRASP compare with DARC and AUTOSTRUCTURE[43].

Index	Term	Parity	J	GRASP	Breit + QED	DARC	A.S.
1	$2s^2 2\bar{p}^2 2p^3(^2P)$	O	3/2	-.4720987E+03	.13410E+00	-.4670541E+03	-.4718731E+03
2	$2s^2 2\bar{p}^1 2p^4(^2P)$	O	1/2	.3193145E-01	-.19469E-02	.2899075E-01	.3795008E-01
3	$2s^1 2\bar{p}^2 2p^4(^2S)$	E	1/2	.3500139E+01	-.14530E-02	.4148588E+01	.3401470E+01
4	$2s^2 2\bar{p}^1 2p^3 3s^1(^4P)$	E	5/2	.6685800E+01	-.50700E-02	.4891984E+01	.7149741E+01
5	$2s^2 2\bar{p}^1 2p^3 3s^1(^4P)$	E	3/2	.6705759E+01	-.52620E-02	.4910496E+01	.7170575E+01
6	$2s^2 2p^4 3s^1(^4P)$	E	1/2	.6717852E+01	-.58040E-02	.4921561E+01	.7183085E+01
7	$2s^2 2\bar{p}^1 2p^3 3s^1(^2P)$	E	3/2	.6806764E+01	-.50820E-02	.5059006E+01	.7276561E+01
8	$2s^2 2\bar{p}^1 2p^3 3s^1(^2P)$	E	1/2	.6830757E+01	-.56280E-02	.5081283E+01	.7301580E+01
9	$2s^2 2\bar{p}^2 2p^2 3s^1(^2D)$	E	5/2	.7111887E+01	-.57890E-02	.5410054E+01	.7556048E+01
10	$2s^2 2\bar{p}^2 2p^2 3s^1(^2D)$	E	3/2	.7112110E+01	-.57280E-02	.5410214E+01	.7556331E+01
11	$2s^2 2\bar{p}^2 2p^2 3s^1(^2S)$	E	1/2	.7680217E+01	-.37900E-02	.6116256E+01	.8089801E+01

The absorption oscillator strength f_{ij} and radiative rate A_{ji} for an allowed transition $i \to j$ are related by eq.(18),where S is the line strength.Table (4) explain the present transition energies ΔE_{ij}(Ang.), oscillator strengths f_{ij} , radiative rate $A_{ji}(\sec^{-1})$ and line-strength S_{ji} (a.u.) obtained from GRASP in length form only, for all the 16 electric dipole (E1) allowed transitions among the 11 levels of Al^{+4}. The present results are compared with the results obtained by using the atomic structure code AUTOSTRUCTURE[43] where the AUTOSTRUCTURE[43] results obtained by using the theoretical transition energies and the same configurations for target or core ion Al^{+4} that were employed to determine the energies for AUTOSTRUCTURE[43] as listed in table (3). The present results obtained by using the fully relativistic GRASP code[36],Some of the AUTOSTRUCTURE [43] results agree well with the GRASP calculations, but for other transitions, they have the same behavior with transition energy ,so the results are in good agreement.The indices used to represent the lower and upper levels of a transition have been defined in table (3). While calculating the oscillator strengths and radiative rates, the QED plus Breit corrected energies are used in the calculations as listed in table (3).

Table (4): Transition energies ΔE_{ij}(Ang.), radiative rates $A_{ji}(\sec^{-1})$,oscillator strengths f_{ij} and line-strength S_{ji}(a.u.) of Al^{+4}obtained from GRASP are compared with the results obtained by using the atomic structure code AUTOSTRUCTURE[43].

		GRASP				A.S.		
i	j	ΔE_{ij}	A_{ji}	f_{ij}	S_{ji}	A_{ji}	f_{ij}	S_{ji}
1	3	.7971E+03	.2404E+11	.1223E+00	.4194E+00	.2459E+11	.2646E+00	.4668E+00
1	4	.1522E+04	.1446E+08	.6050E-04	.1087E-03	.2651E+08	.1937E-03	.1630E-03
1	5	.1527E+04	.2011E+09	.5575E-03	.9985E-03	.3302E+09	.1599E-02	.1338E-02
1	6	.1529E+04	.3796E+07	.5246E-05	.9378E-05	.8523E+07	.2057E-04	.1700E-04
1	7	.1550E+04	.2178E+11	.5861E-01	.1034E+00	.3659E+11	.1721E+00	.1419E+00
1	8	.1555E+04	.8853E+10	.1183E-01	.2080E-01	.1502E+11	.3508E-01	.2883E-01
1	9	.1619E+04	.9723E+10	.3596E-01	.6072E-01	.1608E+11	.1052E+00	.8353E-01
1	10	.1619E+04	.1128E+10	.2781E-02	.4697E-02	.1612E+10	.7030E-02	.5582E-02
1	11	.1749E+04	.4631E+10	.4892E-02	.7647E-02	.8236E+10	.1566E-01	.1162E-01
2	3	.7902E+03	.1167E+11	.1208E+00	.2089E+00	.1189E+11	.1308E+00	.2333E+00
2	5	.1520E+04	.1774E+08	.9928E-04	.8930E-04	.2656E+08	.1299E-03	.1090E-03
2	6	.1522E+04	.5019E+08	.1399E-03	.1257E-03	.8136E+08	.1984E-03	.1670E-03
2	7	.1543E+04	.3746E+10	.2034E-01	.1802E-01	.6021E+10	.2862E-01	.2372E-01
2	8	.1548E+04	.1688E+11	.4550E-01	.4018E-01	.2804E+11	.6615E-01	.5465E-01
2	10	.1612E+04	.8711E+10	.4331E-01	.3673E-01	.1438E+11	.6335E-01	.5057E-01
2	11	.1742E+04	.2740E+10	.5833E-02	.4577E-02	.5119E+10	.9830E-02	.7325E-02

The number of continuum orbitals per angular momentum for the wave function of the target or core ion Al^{+4} is equal to 20 , the R-matrix boundary equal to 4.92 a.u. and the arbitrary constant b of eq.(9) is zero. The calculated ionization energy for Al^{+3} ion by DARC is 6.30514 a.u. compare with 6.09449 a.u. obtained from the atomic structure code AUTOSTRUCTURE[43].The total cross section leave the residual core ion in all accessible target states ,where it is of a given state corresponds to the sum of the partial photoionization cross sections in to the ground state as well as the excited states of the residual core ion.Figure (4) shows the total photoionization cross section of Al^{+3} ion in the length and velocity gauge obtained by eq.(16) in the photon energy rage of 10 to 30.0 rydberg which covers all the thresholds in the Al^{+4} target states, and the resonances of the dominant Rydberg series can be seen clearly for the present results.The present results are compared with the theoretical results of Jha et.al. [46],where these results obtained by using 68 target states of Al^{+4} ion with Breit-Pauli R-matrix method.The present length and velocity results are in good agreement with each other ,the resonance positions of Jha et.al. [46] results tend to small energy compare with the resonance positions of our results,but in general all the results have the similar behavior with energy.This agreement is due to core excitations ,where they are formed due to doubly excited rydberg states converging to core thresholds.The resonance peak appear when the excitation threshold is approached and drop almost to minimum as photon energy is used for excitation and electron is released .In general the agreement is satisfactory for the present calculations.

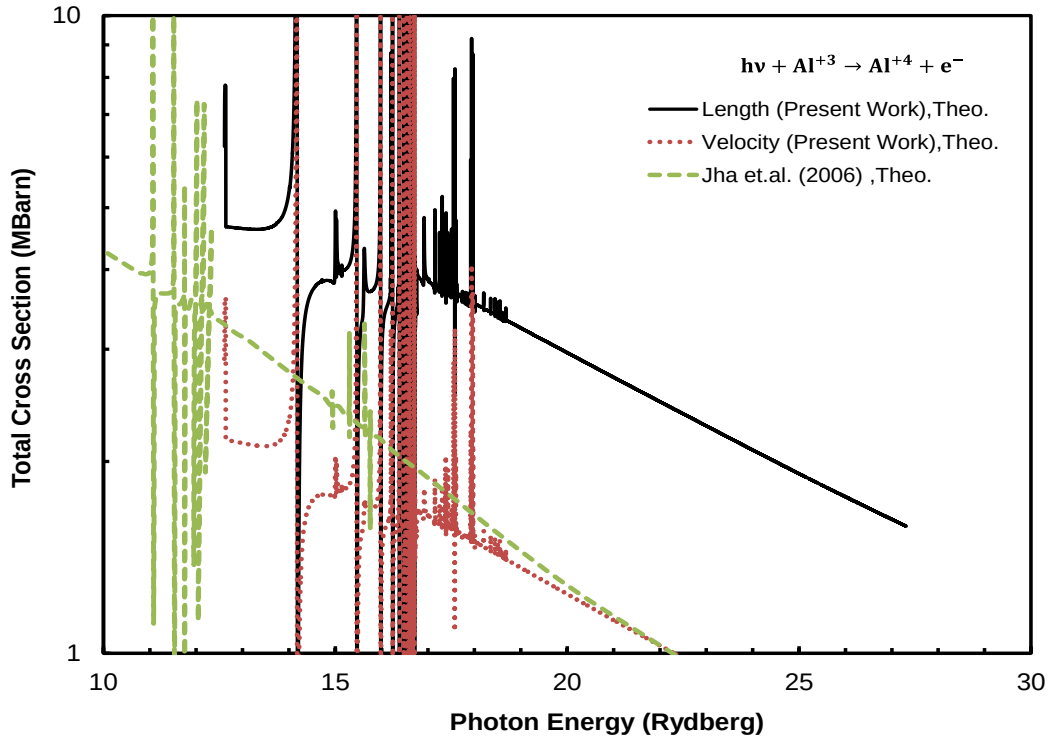

Figure (4) : Total photoionization cross section of Al^{+3} ion in the length and velocity gauge.

According to the results of photoionization cross section of Al^{+3} ion,the recombination cross sections , can be obtained in length and velocity forms $\sigma_{RC}^{L,V}$ by using eq.(17), according to the principle of detailed balance or Milne relation [39]. Figure (5) shows the total recombination cross section of $(e^- + Al^{+4} \rightarrow Al^{+3} + h\nu)$ processes in the photon energy range of 12.5 to 20.0 rydberg ,the comparison here is made between length and velocity gage, the recombination cross section diverges at 12.61 rydberg of photon energy where this energy is equal to ionization energy for Al^{+3} ion, and then it decays with energy until resonance appears at increases energies. The resonance appears on the $n = 2$ and $n = 3$ threshold of core Al^{+4} ion , where the resonance represents the capture of electron,the resonance peak appears when the excitation threshold is approached and drop almost to minimum as photon energy is used for excitation and electron is released,these resonance complexes are according to core excitations,where they are formed according to doubly excited rydberg states converging to core thresholds [45]. In general the resonance can be observed in the recombination spectra as a peak lines .There is a good agreement for the present target states calculations between the length and velocity gage which covers the thresholds in the Al^{+4} ion target states.

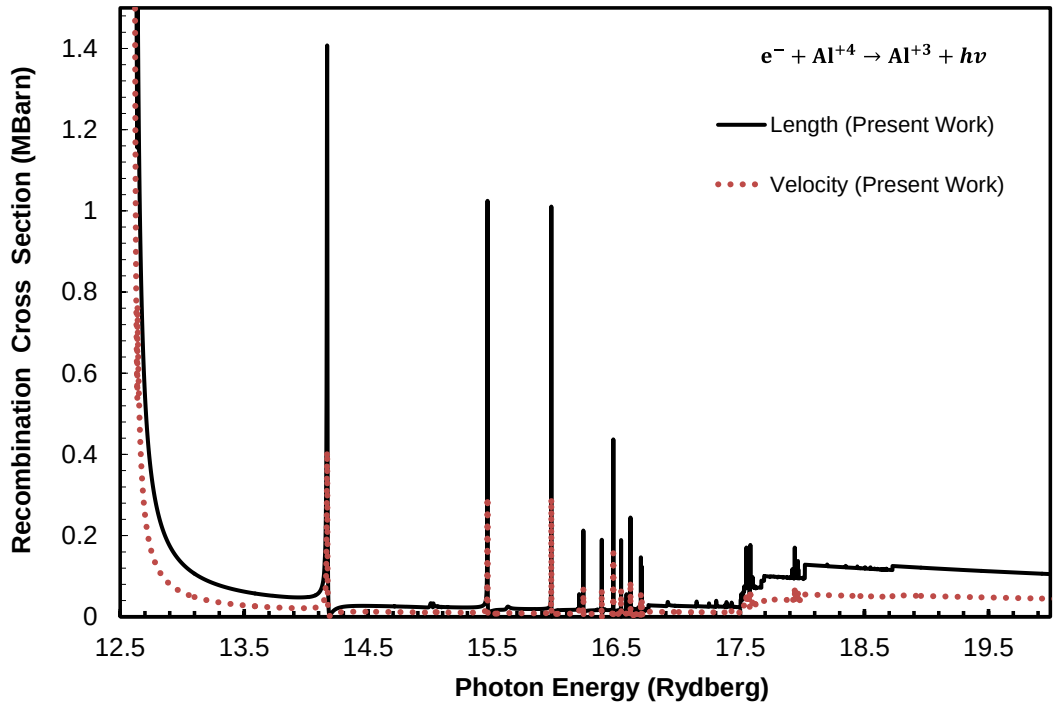

Figure (5) : Total recombination cross section of $(e^- + Al^{+4} \rightarrow Al^{+3} + h\nu)$ in the length and velocity gauge using 11 target states .

The total recombination cross-sections and the recombination rates are related to each other according eq.(20) through the velocity of photoelectron and hence show similar detailed resonant features. Figure (6) shows the total photo-recombination rates of $(e^- + Al^{+4} \rightarrow Al^{+3} + h\nu)$ process in the photon energy range of 12.5 to 20.0 rydberg.The calculated rates show detailed resonant structures similar to that of figure (5),where the recombination rates diverges at 12.61 rydberg of photon energy. The

resonance appears on the $n = 2$ and $n = 3$ thresholds of the recombination rates and can be observed in the recombination rates spectra as peak lines as discussed in figure (5). There is a good agreement for the present target states calculations between the length and velocity gage which covers the thresholds in the Al^{+4} ion target states.

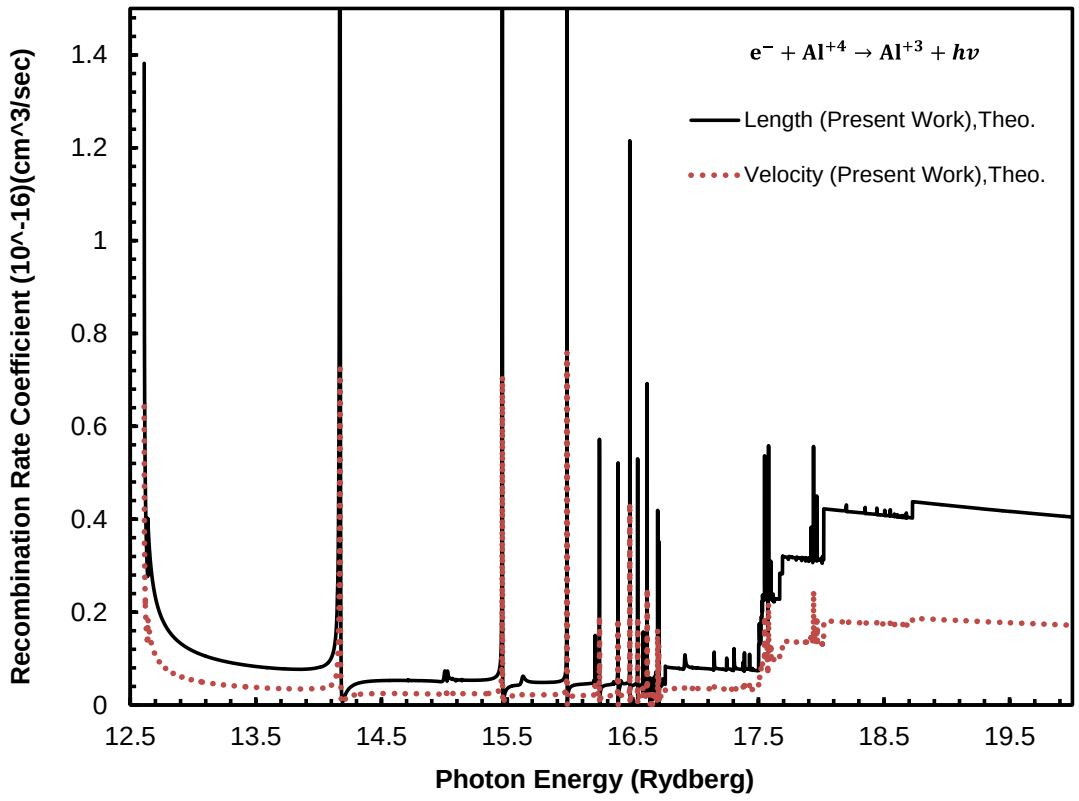

Figure (6): Total recombination rates of $(e^- + Al^{+4} \rightarrow Al^{+3} + h\nu)$ in the length and velocity gauge using 11 target states .

4. Conclusion

Energy levels,the absorption oscillator strength , radiative rate for an allowed transition and line strength for E1 transition,as well as the Photoionization and electron-ion recombination of N^{+1} and Al^{+3} ions are investigated using the fully relativistic R-matrix method .These processes are fundamental atomic processes in astrophysical plasmas.The Dirac Atomic R-matrix Code has been used to handle bound states , photoionization, radiative recombination and other radiative processes . A relativistic atomic structure program GRASP is used to obtain bound orbitals from which the target ions are constructed in Dirac atomic R-matrix code DARC. Further relativistic contributions to the atomic states due to Breit interactions are added by diagonalizing the Dirac-Coulomb-Breit Hamiltonian matrix.The dominant quantum electrodynamic contibutions have also been included as a perturbation.Calculations have been performed on N^{+1} and Al^{+3} ions where the results obtained include the energy of levels ,the oscillator strength (f_{ij}) , radiative rates (A_{ji}),line strength (S_{ij}) for an electric dipole allowed transitions, photoionization, photo-recombination cross-sections and recombination rates. The

results for ground state energy and excitation energies of N^{+2} and Al^{+4} ions by using GRASP , DARC and AUTOSTRUCTURE are in good agreement with each other while the results for absorption oscillator strength f_{ij} , radiative rate A_{ji} for an allowed transitions and the line strength of N^{+2} and Al^{+4} ions are obtained by using the fully relativistic GRASP code and compared with the results obtained by using the atomic structure code AUTOSTRUCTURE where some of the AUTOSTRUCTURE results agree well with the GRASP calculations, but for other transitions, they have the same behavior with transition energy .The results of total photoionization cross section of N^{+1} ion in the length and velocity gauge agree with theoretical results of Nahar and Pradhan ,where they have the similar behavior with energy. Also,the total photoionization cross section of Al^{+3} ion in the length and velocity gauge are compared with the theoretical results of Jha et.al.,where the last results obtained by using 68 target states of Al^{+4} ion with Breit-Pauli R-matrix method, the present length and velocity results are in good agreement with each other ,the resonance positions of Jha et.al. results tend to small energy compare with the resonance positions of our results,but in general all the results have the similar behavior with energy.This agreement is due to core excitations ,where they are formed due to doubly excited rydberg states converging to core thresholds.The resonance peak appear when the excitation threshold is approached and drop almost to minimum as photon energy is used for excitation and electron is released as explained in the results of recombination cross section and recombination rate coefficients for N^{+1} and Al^{+3} ions.In general the agreement is satisfactory for the present calculations.

References

[1] J.B.West, J. Phys. B 34 (2001) R45.
[2] M.J. Seaton, J. Phys. B 20 (1987) 6363.
[3] K.A.Berrington et.al., J. Phys. B20 (1987) 6379.
[4] O.Zatsarinny, Comput. Phys. Comm.,174 (2006) 273–356.
[5] A. Einstein. Ann. Phys. (Leipzig), **17**, 132 (1905).
[6] H. Hall. Rev. Mod. Phys. **8**, 358 (1936).
[7] H.A.Bethe and E.E.Salpeter, Quantum mechanics of one and two-electron atoms. Springer-Verlag, Berlin. 1958. p. 299.
[8] U. Fano and J.W. Cooper. Rev. Mod. Phys. 40, 441 (1968).
[9] A.F. Starace. Handbuch der Physik. Vol. 31. Edited by W. Mehlhorn, Springer-Verlag, Berlin. 1982. pp. 1–121.
[10] R.McWhirter and H.Summers, Applied Atomic Collision Physics (Academic, New York, 1983).
[11] E. I. Moses, R. N. Boyd, B. A. Remington, C. J. Keane, and R. Al Ayat, Phys. Plasmas 16, 041006 (2009).
[12] V. Schmidt, Rep. Prog. Phys. 55, 1483 (1992).
[13] H. S. Chakraborty, PRAMANA journal of physics,Vol.50,No.6, pp. 607(1998).
[14] N.S.Scott, Comput. Phys. Comm., 180 (2009) 2424–2449.
[15] P.G. Burke, K.A. Berrington (Eds.), Atomic and Molecular Processes and R-Matrix Approach, IOP Publishing, Bristol, 1993.
[16] P.G. Burke, C.J. Noble, V.M. Burke, Adv. At. Mol. Opt. Phys. 54 (2007) 237.
[17] E.P. Wigner, Phys. Rev. 70 (1946) 15.
[18] E.P. Wigner, Phys. Rev. 70 (1946) 606.
[19] P.G. Burke, Computational Physics, Inst. Phys. and Phys. Soc., London (1970) 9 .
[20] D.C.S. Allison, Comput. Phys. Comm. 1 (1969) 16.
[21] P.G. Burke, Comput. Phys. Comm. 1 (1969) 241.

[22] A. Hibbert, Comput. Phys. Comm. 1 (1970) 359.
[23] W.D. Robb, Comput. Phys. Comm. 1 (1970) 457.
[24] W.D. Robb, The calculation of atomic properties, Ph.D. thesis, The Queen's University of Belfast, 1971.
[25] K.A. Berrington, P.G. Burke, J.J. Chang, A.T. Chivers, W.D. Robb, K.T. Taylor,Comput. Phys. Comm. 8 (1974) 149.
[26] K.A. Berrington, P.G. Burke, M. Le Dourneuf, W.D. Robb, K.T. Taylor, V.K. Lan, Comput. Phys. Comm. 14 (1978) 367.
[27] N.S. Scott, K.T. Taylor, Comput. Phys. Comm. 25 (1982) 347.
[28] P.G. Burke, V.M. Burke, N.S. Scott, Comput. Phys. Comm. 69 (1992) 76.
[29] K.A. Berrington, W.B. Eissner, P.H. Norrington, Comput. Phys. Comm. 92 (1995) 290.
[30] K.A. Berrington, P.G. Burke, K. Butler, M.J. Seaton, P.J. Storey, K.T. Taylor, Yu. Yan, J. Phys. B: At. Mol. Phys. 20 (1987) 6379.
[31] M.J. Seaton, J. Phys. B: At. Mol. Phys. 20 (1987) 6363.
[32] D.G. Hummer, K.A. Berrington, W. Eissner, A.K. Pradhan, H.E. Saraph, J.A. Tully, Astron. Astrophys. 279 (1993) 298.
[33] P.G.Burke, A.Hibbert and W.D.Robb , J. Phys. B 4 (1971)153.
[34] P.H. Norrington and I.P.Grant, J. Phys. B 20 (1987)4869.
[35] W.P. Wijesundera et.al., J. Phys. B 24 (1991)1803.
[36] P.H. Norrington, I.P. Grant, online at http://www.am.qub.ac.uk/DARC/.
[37] P.G. Burke, A.Hibbert and W.D.Robb, J. Phys. B: At. Mol. Phys. 4 (1971) 153.
[38] J.J.Chang, J. Phys. B: At. Mol Phys. 8 (1975) 2327.
[39] S.N.Nahar, The Astrophysical Journal Supplement Series, 156(2005)93–103.
[40] S. N. Nahar, Atomic Data and Nuclear Data Tables 80, (2002) 205–234.
[41] S.N.Nahar,Journal of Quantitative Spectroscopy & Radiative Transfer 110 (2009) 2148–2161.
[42] K.M. Aggarwala and F.P. Keenan, Eur. Phys. J. D 46, (2008) 205–213.
[43] N.R.Badnell, Comput. Phys. Comm. 182 (2011) 1528-1535.
[44] S.N.Nahar and A.K.Pradhan, The Astrophysical Journal Supplement Series,111 (1997)339.
[45] S.N.Nahar,New Astronomy,15(2010) 417-426.
[46] A.K.S. Jha,P. Jha,S.Tyagi, and M. Mohan, Eur. Phys. J. D 39, 391–398 (2006).

ألتاين ألضوئي, أعادة المزج بين ألالكترون وألايون ومعدل أعادة المزج لأيونات N^{+1} و Al^{+3} بأستخدام ألطريقة ألنسبية لمصفوفة ألبعد لديراك

عقيل هاشم حسين علاء عبد الحسن خلف فلحي عبد ألحسن علي

قسم الفيزياء/ كلية العلوم/ جامعة البصرة

البريد الالكتروني : akeel_hashem74@yahoo.com

ألخلاصة

تم دراسة ألتاين ألضوئي وأعادة المزج بين ألالكترون وألايون والعمليات ألاشعاعيه لايونات N^{+1} و Al^{+3} باستخدام ألطريقة ألنسبية لمصفوفة ألبعد لديراك.هذه العمليات هي عمليات ذرية أساسيه.في اكثر النماذج سابقا هذه المقادير الذرية لا تمثل بصورة كافية مستوى المشاركة لعدد كبير من عمليات الرنين التلقائية الموضحة في مقاطع التاين الضوئي واعادة المزج بين الالكترون والايون .ان ألطريقة ألنسبية لمصفوفة ألبعد لديراك امتدت وتوسعت من عمليات استطارة الكترون الطاقة الواطئه لتشمل الحالات المقيده والتاين الضوئي واعادة المزج.أن الدوال الموجية للمدارات في الحسابات النسبية لمصفوفة البعد لديراك يتم الحصول عليها من طريقة ديراك–فوك المتعددة المساهمة وذلك باستخدام البرنامج الدولي(GRASP). حيث في هذه الطريقة دالة الحالة الذرية تقرب بواسطة المزج الخطي لدوال تشكيل الحالة ذات نفس التناظر.أن دوال تشكيل الحالة هي حاصل ضرب غير متناظر لمجموعة مشتركة من المدارات المتعامدة–العيارية والتي مجموعها تشكل دوال اساسية للمؤثر الهاملتوني لديراك–كولوم .هذة الدوال ألاساسية تستخدم لايجاد دوال المدارات المقيده الداخلة بتركيب ايون الهدف والذي يستخدم بالحسابات باستخدام البرنامج (DARC).تم اضافة تاثيرات نسبية أضافية للحالات ألذرية طبقا لتفاعلات بريت وذلك بجعل المصفوفة الهاملتونية لديراك–كولوم–بريت مصفوفة قطرية.أن الحسابات انجزت على ايونات N^{+1} و Al^{+3} حيث تم الحصول على اتفاق جيد بين النتائج في هذا البحث مع نتائج الباحثين الاخرين .

كلمات مفتاحية : ألتاين ألضوئي , أعادة مزج ألكترون–ايون , معادلة ديراك , طريقة مصفوفة البعد النسبية